Short-term response of bone related markers over stimulatory and resting periods – case series conducted on sheep.

J. Barcik[1], M. Ernst[1], T. Buchholz[1], C. Constant[1], S. Zeiter[1], S. Verrier[1]

[1]AO Research Institute Davos, AO Foundation, Davos, CH

INTRODUCTION: The importance of mechanical stimulation in secondary bone healing is well-established. However, recent animal studies have suggested that the resting period between stimulation cycles might be a crucial – but so far underestimated – parameter that impacts fracture healing [1-2]. Our objective is to determine the blood levels of factors associated with bone formation and bone resorption during the active and resting phases of bone stimulation.

METHODS: Upon local ethics committee approval (TVB2020/26 Canton of Grisons, CH), six Swiss White Alpine sheep underwent partial osteotomy of a tibia that was stabilised with an active fixator. The active fixator applied 1000 loading cycles per day evenly distributed from 9 am to 9 pm (12-hours stimulation period), followed by 12 hours of rest. On day 22 and day 29 post-surgery, blood samples were taken at three key time points: 9 am (start of stimulation period), 9 pm (start of resting period) and 9 am next day (start of a new stimulation period) – Fig 1. For pre-operative baseline measurement, blood samples were taken following the same schedule. After plasma separation, blood samples were analysed for the concentration of bone formation markers: bone alkaline phosphatase (BAP), osteocalcin (OC) and bone remodelling marker type 10 collagen using enzyme-linked immunosorbent assay (ELISA, neobiolab). We evaluated the changes of markers over stimulation and over resting using equations 1 and 2.

$$\Delta_{stimulation} = \frac{(x_{9_{pm}} - x_{9_{am}})}{x_{9_{am}}} 100\% \quad (1)$$

$$\Delta_{Resting} = \frac{(x_{9_{am\_next\_day}} - x_{9_{pm}})}{x_{9_{pm}}} 100\% \quad (2)$$

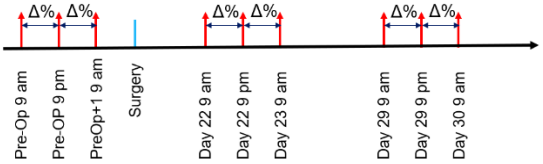

Fig. 1: Blood taking timepoints. Δ% indicates which timepoints were compared.

$\Delta_{stimulation} = \frac{(x_l - x_f)}{x_f} 100\%$ **RESULTS:** All animals tolerated the active fixation and the stimulation protocol well. We observed that during the healing process, the levels of BAP and OC mainly increased during the resting phase – Table 1. For both markers, no clear pattern was observed at the base line measurements. A similar pattern was observed for type 10 collagen over healing; and to some extent baseline levels seems to be also sensitive to circadian rhythm (base line level) – Table 1.

Bone Alkaline Phosphatase (BAB)					
pre-OP		Day 22		Day 29	
9 am - 9 pm	9 pm - 9 am next day	9 am - 9 pm	9 pm - 9 am next day	9 am - 9 pm	9 pm - 9 am next day
[%]	[%]	Δ stimulation [%]	Δ rest [%]	Δ stimulation [%]	Δ rest [%]
-0.004	0.085	-0.241	0.111		-0.019
8.570	-5.871	-9.197	15.943	-17.419	10.316
-16.028	1.351	-3.956	14.186	-7.146	2.111
-0.512	-5.553	-8.632	8.014	-15.038	11.239
-16.947	1.704	-1.523	18.166	7.424	4.638
2.803	-6.518	20.313	-14.280	-0.986	14.657
Osteocalcin (OC)					
pre-OP		Day 22		Day 29	
9 am - 9 pm	9 pm - 9 am next day	9 am - 9 pm	9 pm - 9 am next day	9 am - 9 pm	9 pm - 9 am next day
[%]	[%]	Δ stimulation [%]	Δ rest [%]	Δ stimulation [%]	Δ rest [%]
27.662	-4.273	-8.007	12.132	4.809	15.121
-55.427	98.706	11.994	14.403	7.525	18.458
26.989	-10.693	-3.988	29.487	-9.712	6.811
-23.039	-2.818	12.856	0.372	-5.123	13.126
-20.794	-4.214	46.609	-24.509	-1.234	-13.547
Type 10 collagen					
pre-OP		Day 22		Day 29	
9 am - 9 pm	9 pm - 9 am next day	9 am - 9 pm	9 pm - 9 am next day	9 am - 9 pm	9 pm - 9 am next day
[%]	[%]	Δ stimulation [%]	Δ rest [%]	Δ stimulation [%]	Δ rest [%]
-6.379	5.616	10.141	-3.547	-2.108	15.750
-13.054	-1.263	-1.964	9.916	-16.422	6.586
-9.267	22.773	-53.247	117.399	-6.611	-16.327
4.820	-19.998	-2.626	9.247		2.552
-17.965	29.193	-13.342	37.236	-8.092	16.353
-23.591	22.325	14.988	8.719	-2.133	19.215

Table 1. effect of stimulation or resting period of sheep osteotomies on BAP, OC and type 10 collagen levels in plasma.
Results were calculated as shown in Fig1. Green: upregulation, yellow: downregulation.

DISCUSSION & CONCLUSIONS: The presented data suggests that the bone formation process – characterised by the levels of BAP and OC – occurs mainly during the resting periods. These preliminary findings emphasize further the importance of resting periods between stimulatory events as a crucial parameter impacting fracture healing progression.

ACKNOWLEDGEMENTS: This study was performed with the assistance of the AO Foundation via the AOTRAUMA Network (Grant No.: AR2019_06)

REFERENCES: [1] Barcik, Jan, et al. Biomedicines 9.8 (2021): 988.
[2] Hente, R., and S. M. Perren. Acta Chir. Orthop. Traumatol. Cech 85 (2018): 385-391.

Contrast-enhanced ultrasound imaging of displaced humeral fractures: Results of a pragmatic single-centre study.

D. Cadoux-Hudson[1], M.Thomas[1], J.Hurst[1], R.Schranz[1], A.Gerrish[1], K.Wallace[3], D.Warwick[1], D.Carugo[4], Stride E[4], S.Tilley[1], N.D.Evans[2]

[1]University Hospitals Southampton, UK; [2]University of Southampton,UK; [3]GE Medical Imaging; [4]University of Oxford, UK.

INTRODUCTION: Microbubbles have been commercially available in ultrasonography for the purposes of contrast enhanced imaging for several decades. As the understanding of the properties of microbubbles has improved, so has the scope for their use in a therapeutic setting. Microbubbles have been described in an orthopeadic setting as a method for determining the likely cause of an established non-union in the clinical setting(1). There is, however, little literature describing the behaviour of microbubbles in acute bone fractures, or therefore their potential for therapeutic and diagnostic use in this application. The aim of this study is to determine the ability of microbubbles to perfuse acute fractures in the clinical setting.

METHODS: Patients who had sustained a humeral shaft fracture were recruited to undergo ultrasound enhanced contrast imaging of the fracture site within 28 days of injury. They underwent ultrasound imaging and peripheral injection of commercially available SonoVue (Bracco, Italy) microbubbles. B-mode images were captured together with time-intensity curves to assess presence of microbubbles at the fracture site.

RESULTS: Seven patients underwent ultrasound enhanced contrast imaging of acute humeral fractures with a mean time to scan of 16 days. The average Peak Intensity (PI) was 1.95×10^{-6} acoustic units (AU) with an average Area Under the Curve (AuC) of 4.68×10^{-6} and average Time to Peak (TtP) of 23.4 seconds. There was a noticeable drop in these metrics with increased time from injury, (5 versus 28 days; PI, 70.8%, AuC 62.4% and TtP 20.3%). There was a significant flow of microbubbles confined to within the fracture site and within the callus itself, as shown in Figure 1, which demonstrates microbubble contrast within the fracture site outlined.

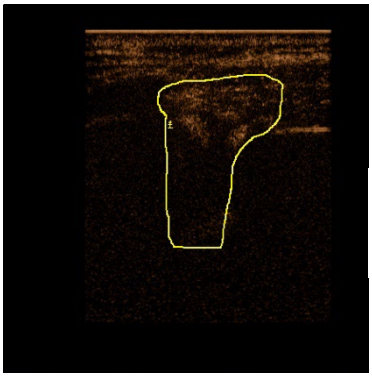

Figure 1: Microbubble contrast in acute humeral fracture

DISCUSSION & CONCLUSIONS This preliminary human clinical study demonstrates the presence of peripherally injected microbubbles in acute fractures. This demonstrates the viability of using microbubbles for therapeutic purposes and for assessing changes in blood flow through fractures over time from acute injury in clinical settings.

REFERENCES:

1. Fischer C, Haug T, Weber MA, Kauczor HU, Bruckner T, Schmidmaier G. Contrast-Enhanced Ultrasound (CEUS) Identifies Perfusion Differences Between Tibial Fracture Unions and Non-Unions. Ultraschall Med - Eur J Ultrasound. 2020 Feb;41(01):44–51.

Dental Pulp Stem cells facilitate the engineering of 3D functional prevascularized constructs

Eirini Chatzopoulou[1], Nour Bousaidi[1], Thomas Guilbert[2], Guillaume Rucher[3,4], Jimmy Rose[5,6], Stephane Germain[7], François Rouzet[5], Catherine Chaussain[1,8], Laurent Muller[7], Caroline Gorin[1,8]

[1]Université Paris Cité, URP2496, Montrouge, France. [2]Institut Cochin, Plateforme IMAG'IC, Université Paris Cité, Paris, France. [3]Université Paris Cité, LVTS, INSERM U1148, Paris, France. [4]Université Paris Cité, UMS 34 - FRIM, Paris, France. [5]Nuclear Medicine Department, Bichât-Claude Bernard Hospital, APHP, Université Paris Cité, LVTS, INSERM U1148, F-75018, Paris, France. [6]Université Paris Cité, UMS 34 - FRIM, F-75018, Paris, France. [7]Center for Interdisciplinary Research in Biology (CIRB), Collège de France, INSERM U1050, Paris, France. [8]AP-HP, Services Odontologie, GH Paris Nord, France

INTRODUCTION: The concept of prevascularization is a promising strategy for the rapid establishment of a vascular network within bone defects and subsequently, the success of a bone graft. Dental pulp stem cells from deciduous teeth (SHED) demonstrate angiogenic potential and vessel pericyte function[1]. This study describes the fabrication of 3D pre-vascularized SHED cultures in polylactic acid (PLA) scaffolds and explores the *in vivo* integration of the engineered vasculature.

METHODS: Collagen hydrogels were held in PLA grids prior to subcutaneous implantation in nude mice according to the following groups: 1) human endothelial cells (EC) and SHED co-culture (EC-SHED), 2) EC treated with SHED conditioned medium (EC-SHED-CM), 3) SHED alone. Cell viability and capillary parameters were assessed *in vitro* inside the grids. After *in vivo* implantation, early angiogenesis was investigated by positron emission tomography (PET) using a 64Cu-NODAGA-RGD tracer. Mouse (IB4) and human (UEA1) fluorescent lectins were injected, and the explanted constructs were imaged with two-photon microscopy[2]. Finally, the vasculature was analyzed by contrast-enhanced micro-CT acquisition. The PLA grids were further characterized with immunohistochemistry.

RESULTS: The *in vivo* PET at day 10 showed that the radiotracer was significantly increased in the pre-vascularized groups compared to SHED alone, indicating higher angiogenic activity in these groups. After injection of species-specific lectins, multiple anastomoses of human implanted vessels with the host's vessels were detected, highlighting the perfusion of the engineered vessels. The micro-CT revealed a statistically significant increase in the total vascular volume in the EC-SHED group. The presence of human adherent junctions (VE-cadherin), sensitive innervation (cGRP) and the deposition of basement membrane (collagen type IV) suggested the presence of a mature human vascular network.

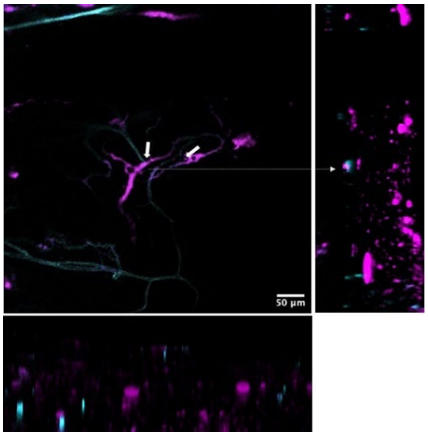

Fig. 1: *Anastomosis of the human implanted vessels (UEA1 lectin in violet) with mouse vessels (IB4 lectin in cyan)*

DISCUSSION & CONCLUSIONS: Apart from the well documented SHED ability to boost the bone healing process, this study supports the interest for pre-vascularization with SHED stem cells before implantation in order to produce a mature microvasculature withing implanted constructs, a key factor for successful bone regeneration.

ACKNOWLEDGEMENTS: This work was supported by Fondation de l'avenir and Fondation pour la Recherche Médicale (PhD EC).

REFERENCES:

1. Atlas, Gorin et al. Biomaterials. 268:120594, 2021

2. Schoenherr, Chatzopoulou et al. iScience. 26:106286, 2023

Micro-porous PLGA/β-TCP/TPU scaffolds prepared by solvent-based 3D printing for bone tissue engineering purposes

Luan P Hatt[1,2], Sylvie Wirth[1,2], Aapo Ristaniemi[1], Daniel J Ciric[1], Keith Thompson[1,3], David Eglin[1,4], Martin J Stoddart[1,5], Angela R Armiento[1,3]

[1]AO Research Institute Davos, Clavadelerstrasse 8, 7270, Davos Platz, Switzerland, [2]Institute for Biomechanics, ETH Zürich, 8093, Zürich, Switzerland, [3]UCB Pharma, 216 Bath Road, SL1 3WE, Slough, United Kingdom, [4]Mines Saint-Étienne, Univ Lyon, Univ Jean Monnet, INSERM, U1059, 42023, Sainbiose, Saint-Étienne, France, [5]Medical Center-Albert-Ludwigs-University of Freiburg, Faculty of Medicine, Albert-Ludwigs-University of Freiburg, 79106 Freiburg, Germany

INTRODUCTION: The 3D printing process of fused deposition modelling (FDM) is an attractive fabrication approach to create tissue engineered bone substitutes to regenerate large mandibular bone defects, but often lacks desired surface porosity for enhanced protein adsorption and cell adhesion. Solvent-based printing leads to the spontaneous formation of micropores on the scaffold's surface upon solvent removal, without the need for further post processing. The aim of this study is to create and characterise porous scaffolds using a new formulation composed of mechanically stable poly(lactic-co-glycol acid) (PLGA) and osteoconductive β-tricalcium phosphate (β-TCP) with and without the addition of elastic thermoplastic polyurethane (TPU) prepared by solvent-based 3D-printing technique.

METHODS: 40% (w/v) of PLGA and 20% (w/v) of β-TCP are mixed with or without 10% of TPU (w/v) in the solvent ethylene carbonate (EC) to obtain a printable ink. After the printing of a macroporous scaffold using the RegenHu Discovery® printer and water-mediated EC removal, surface microporosity, mechanical properties and cytotoxicity, as well as osteogenic differentiation of human bone marrow-derived stromal cells (hBM-MSCs, obtained with full ethical approval) after 28 days is assessed using µ-CT scanning, SEM, mechanical testing, CellTiter-Blue®, alkaline phosphatase (ALP) assay and OsteoImage™ mineralization staining.

RESULTS: Large scale regenerative scaffolds can be 3D-printed with adequate fidelity and show porosity at multiple levels (Figure 1A). Superior mechanical properties compared to a commercially available CaP ink (OsteoInk®) are demonstrated in compression and bending tests (Figure 1B). Cell metabolic activity assay proves the scaffold's cytocompatibility (Figure 1C). Osteoconductive properties of PLGA/β-TCP scaffold are demonstrated by increased ALP activity and stained area of mineral deposition under osteogenic conditions compared to the osteocontrol condition (Figure 1D).

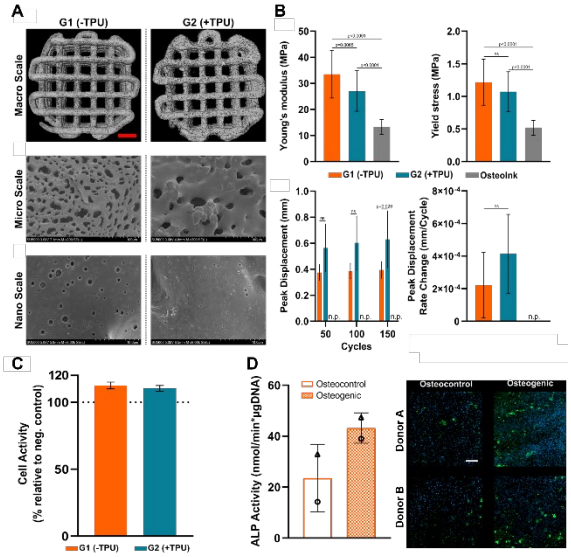

Figure 1. A)µCT and SEM images of 3D-printed scaffolds of three porosity levels (macro, micro, nano), scale bar = 1.5 mm, B) Compression tests (Young's – , yield modulus) and Bending tests (peak displacement, peak displacement rate change), C) Cell metabolic activity and D) Osteogenic assessment of hBM-MSCs (Alkaline Phosphatase (ALP) activity normalized to DNA content at day 14, mineral deposition (green) and nucleus (blue) at day 28, scale bar = 200 µm).

CONCLUSIONS: We propose a versatile fabrication process to create porous 3D-printed scaffolds with adequate mechanical stability and osteoconductivity, both important characteristics for segmental mandibular bone.

ACKNOWLEDGEMENTS: This work was supported by AO CMF and AO Foundation.

Enhanced osseointegration using biomimetic laser-textured implants

W Lackington[1], B Bellon[2], P Schweizer[3], A Ambeza[4], AL Chopard-Lallier[5], A Armutlulu[2], P Schmutz[6], X Maeder[3] and M Rottmar[1]

[1]Biointerfaces Lab, Empa, St. Gallen, CH. [2]Institut Straumann AG, Basel, CH. [3]Mechanics of Materials & Nanostructures Lab, Empa, Thun, CH. [4]Laser TSE, Georg Fischer Machining Solutions SA, Geneva, CH. [5]Anthogyr SAS, Sallanches, FR. [6]Joining Technologies & Corrosion Lab, Empa Dübendorf, CH.

INTRODUCTION: In modern oral maxillofacial surgery, long-term implant stability is intrinsically linked to the quality of osseointegration. The stochastic nature of commonly used implant surface modification techniques, including sandblasting and acid etching, precludes precise control over the uniformity and consistency of the resulting implant surface features. Femtosecond laser-texturing has emerged as an up-and-coming alternative that enables the production of designer surfaces with micro- and nano-scale surface features defined in size and arrangement, which would allow to mimic the multiscale structures of trabecular bone. The aims of this study were therefore to develop a biomimetic laser-textured implant surface, to investigate the influence of laser-texturing on its physicochemical properties, to evaluate its blood-material interface, and to assess its osseointegration capacity *in vitro* and *in vivo*.

METHODS: TiZr samples (Ø5 mm discs and rods) were laser-textured (Laser) using a femtosecond laser system and compared to sandblasted and acid etched TiZr samples (SLA/SLActive). Laser textured samples were boiled (B) to improve their wettability. Samples were incubated with blood and the adsorption of fibrinogen and fibrin network formation was assessed using confocal laser scanning microscopy (CLSM). Bone progenitor cells (HBCs) were seeded on samples pre-incubated with blood, and mineralization was evaluated using calcium quantification assays (n=5). Biomechanical pull-out tests were performed after 4 weeks of implantation into rabbit tibia (n=8). Abiological pull-out tests were performed using a synthetic resin to decouple the influence of the surface architecture and the bio logical response (n=3).

RESULTS & DISCUSSION: The surface of TiZr laser samples featured an organized trabeculae-like microarchitecture superimposed over nano-scale laser induced periodic surface structures. Boiling increased the wettability of Laser surfaces, which led to enhanced fibrin network formation (*Fig. 1A*). Laser outperformed SLActive in terms of supporting *in vitro* mineralization (*Fig. 1B*). Similarly, biomechanical pull-out tests confirmed that implant osseointegration was ~2.5-fold enhanced in rabbits treated with Laser in comparison to SLA. Abiological pull-out tests showed an inferior response to Laser implants, suggesting that the enhanced osseointegration observed was mainly driven by the biological response to the surface.

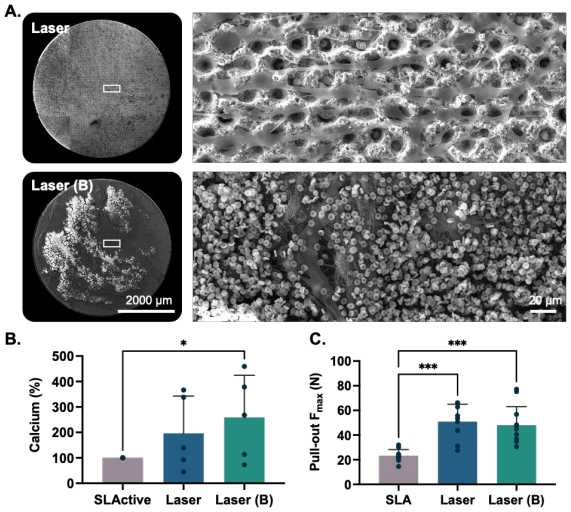

Fig. 1: a) Scanning electron micrographs of Laser and Laser (B) surfaces pre-incubated with blood and seeded with HBCs. b) In vitro mineralization after 28 days. c) In vivo biomechanical pull-out after 4 weeks.

CONCLUSIONS: Notably, this study presents a lean manufacturing alternative to traditional sandblasting and acid etching, for the production of TiZr implants with enhanced osseointegration capacity.

ACKNOWLEDGEMENTS: This research was carried out in the framework of project SOFT 40048.1 IP-LS, supported by Innosuisse – Swiss Innovation Agency.

Femoral neck fracture care in Latin America

Verena Oberlohr, Madeline MacKechnie, Patricia Robles, Michael J. Flores, Marcelo Rio, Sergio Iriarte, Vincenzo Giordano, Jose Eduardo Quintero, David Escalante, José Arturo Xicará, Luis Padilla, Dino Aguilar, Julio Segovia, Igor Escalante, Theodore Miclau, on behalf of the ACTUAR Hip Fracture Study Group

Purpose

The incidence of hip fractures continues to increase throughout Latin America. Despite this, there are few studies that assess hip fracture management in the region, impeding efforts to develop cost-effective solutions for this growing problem. This study seeks to evaluate pre-operative femoral neck fracture management from surgeon-experts in the region.

Methods

A survey, based on input from a panel of Latin American orthopaedic traumatologists, was developed and placed into REDCap. A snowball survey design was utilized for this study. One surgeon-leader per Latin American country (n=11) identified 10 surgeons in their country who could potentially meet a list of "expert" criteria that included: 1) ≥10 years in practice as an orthopedic surgeon; 2) holding a leadership position on a local (hospital); regional (academic or clinical); or national (academic or clinical) level; 3) treating traumatic musculoskeletal injuries at least 50% of their practice; and 4) completing more than 500 hip fracture cases annually as the primary surgeon. Experts identified 108 potential leaders, who were subsequently sent the survey. Descriptive statistics and Fischer's exact tests were performed using STATA 15.0.

Results

Seventy-eight surgeons responded to the survey, yielding a response rate of 72%, of which 44 surgeons met the inclusion criteria. Countries with at least one identified expert included Argentina, Brazil, Colombia, Cuba, Ecuador, Mexico, Panama, Paraguay, Peru, and Venezuela. Amongst the findings for pre-operative care, a majority of surgeon experts reported utilizing pre-traction for femoral neck fractures (84%) and administering prophylactic antibiotics (95%), which were largely first-generation cephalosporins (88%) administered prophylactically less than one hour before surgery (62%). Of note, surgical delays varied by fixation type, with total hip arthroplasty having the longest surgical delays (70% ≥24 hours), followed by hemiarthroplasty (65% ≥ 24 hours) and internal fixation (34% ≥24 hours). Further, there were significant differences in the administration of prophylactic antibiotics (p=0.022) and timing of antibiotic administration (p=0.002) reported across countries in this region.

Conclusion

Understanding existing treatment patterns for hip fracture care is critical for developing standards and addressing areas for needed improvements. While there were common patterns of management, this study demonstrated a variety of differences in critical aspects of hip fracture care by recognized experts across Latin America. These results not only will guide additional future studies on hip fracture management but will aid in the development of best practice recommendations, identification of differences in treatments, and targeting of interventions to address gaps in care in the region.

Activated CD31$^+$ cells from peripheral blood positively impact osteogenesis

Marie A. Mohn[1], Anke Kadow-Romacker[1], Sevim Yanc[1], Katharina Schmidt-Bleek[1], Wilhelm Gerdes[2], Georg N. Duda[1]

[1]Julius Wolff Institute & Berlin Institute of Health Center for Regenerative Therapies, Berlin Institute of Health @ Charité - Universitätsmedizin, Berlin. [2]Cell.Copedia GmbH, Leipzig

INTRODUCTION:

Delayed healing or non-union affects 10-15% of fractures, causing significant suffering for the individual and high costs for the health-care system. Cell therapy of the early fracture hematoma, with concentrated autologous peripheral blood CD31$^+$ cells, initially modulates the immune reaction at the onset of fracture healing. In certain individuals, an over-shooting inflammation during the early fracture stages is thought to be causative of unsatisfactory healing [1]. CD31 selected cells from peripheral whole blood are depleted of terminally differentiated effector and effector memory T cells (TEMRA). Elevated levels of CD8$^+$ TEMRA, have been shown to correlate with unsatisfactory fracture healing outcome [2]. In a rat model of biologically-impaired healing, application of isolated CD31$^+$ cells improved healing outcome [3]. Immune activation of the CD31$^+$ cell population is essential to exhibit the pro-regenerative capacity of CD31$^+$ cells *in vitro* but is not required *in vivo*. Rather, the inherent inflammation within the fracture hematoma where the CD31$^+$ cells are applied 'automatically' activates their anti-inflammatory competence and enables healing.

METHODS: Isolation of minimally manipulated CD31$^+$ cells from whole blood was performed using a novel technology developed by CellCopedia GmbH, Leipzig, Germany. Purity and enrichment of the CD31$^+$ cells including the depletion of CD8$^+$ TEMRA was monitored by multiparameter flow cytometry. CD31$^+$ cells and PBMC were stimulated using anti-CD3, anti-CD28 and LPS and conditioned medium (CM) was collected. HUVEC tube formation assay on Matrigel was performed to assess the influence on angiogenesis. To measure effects on osteogenic differentiation, primary MSC's were cultured in CM with osteogenic supplements. Calcified matrix was quantified after 12 days in culture by alizarin red staining. Concentrations of various cytokines, growth and inflammatory factors were determined using a custom designed LegendPlex array.

RESULTS: Activated CD31$^+$ cells produce factors that have a profound effect on the osteogenic differentiation of MSC's. The observed increased calcification is significantly higher compared to osteogenic differentiation medium alone (OM) or to donor-matched stimulated PBMC controls (Fig 1). Angiogenesis as measured in the tube formation assay is impaired by factors produced by stimulated PBMC, but not by CD31$^+$ cells. Stimulated CD31$^+$ cells produced higher levels of anti-inflammatory cytokines TGF-ß, IL-10 and IL-1RA, and lower amounts of inflammatory cytokines TNFa and IFNg. VEGF concentrations in CM from CD31$^+$ cells were higher, while GM-CSF was lower.

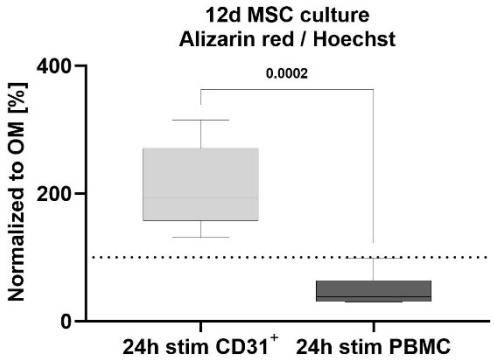

Fig 1: Increased osteogenic differentiation of MSC's induced by culture in conditioned medium from activated CD31$^+$ cells. n=3

DISCUSSION & CONCLUSIONS: Activation of CD31$^+$ immune cells unleashes the natural healing capacity of the cells, allowing them to play their physiological immune modulatory role in the fracture hematoma. Specifically, in patients with TEMRA^{high} such local concentration would be able to enhance healing.

REFERENCES:

1. Hoff, P., et al., Immunol Res, 2016. **64**(5-6): p. 1195-1206.
2. Reinke, S., et al., Sci Transl Med, 2013. **5**(177): p. 177ra36.
3. Sass, F.A., et al., J Bone Miner Res, 2017. **32**(5): p. 902-912.

Influence of testing environment on the degradation behaviour of magnesium alloys for orthopaedic implants

Lavinia Nicolescu [1], Aurora Antoniac[1], Iulian Antoniac[1,2]

[1] Faculty of Material Science and Engineering, University Politehnica of Bucharest, 313 Splaiul Independentei, District 6, 060042 Bucharest, Romania, [2] Academy of Romanian Scientists, 54 Splaiul Independentei, District 5, 050094 Bucharest, Romania

INTRODUCTION: Magnesium (Mg) and its alloys have been extensively researched as a potentially biodegradable implant material. But up until now, the widespread use of Mg-based alloys for implant applications has been hampered by their rapid degradation in physiological environments. The present paper focuses on in vitro degradation of some biodegradable Mg alloys potentially used for orthopedic implants, in different biodegradation environment.

METHODS: The materials used for this research were different magnesium alloys (Mg0.8Ca, ZQ63(MgZn2.5Ag), ZMX410 (MgZn4.3Mn0.6)) in casting state. The microstructural characterization of the experimental samples was made using an Olympus optical microscope (BX51) and a Scanning Electron Microscope QUANTA coupled with energy dispersive X-Ray (EDS). The degradation behaviour of Mg alloys in simulated body fluid (SBF) and Dulbecco's modified eagle medium (DMEM) was evaluated by electrochemical and immersion tests. The electrochemical experiments were performed, under ASTM G5-94 (2011) conditions, using a Potentiostat/Galvanostat (PARSTAT 4000 model, Princeton Applied Research, Oak Ridge, TN, USA) in SBF and DMEM. The determination of the mass loss of the investigated samples was carried out by immersing the experimental samples in Dulbecco's solution and SBF solution and maintaining them for different periods of time in a thermostatic bath (Immersion Bath Circulator LabTech Model LCB-11D) .

RESULTS: The results showed that the lowest hydrogen release rate at the measured time intervals was obtained for ZQ63 alloy. ZMX410 alloys and Mg0.8Ca alloy recorded the highest hydrogen release rate, after 24 hours already exceeding the limit tolerated by the human body (2.25 ml/cm²/day). The high rate of hydrogen release in the case of ZMX410 and Mg0.8Ca alloys is due to the presence of calcium in their composition, an element that is distributed in the structure at the grain boundary and which, in the investigated environments, favours the appearance of cracks accelerating the corrosion process.

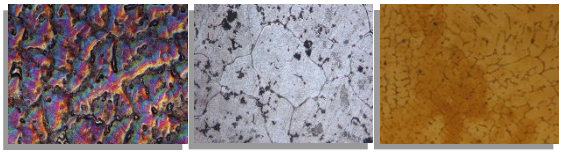

a) b) c)

Fig. 1: Optical microscopy images of the experimental Mg alloys: a) ZQ63 b) ZMX410 c) Mg0.8Ca

DISCUSSION & CONCLUSIONS: The objective of this paper was to present a systematic investigation on different Mg alloys from different system. The positive influence of silver in increasing corrosion resistance is observed in the case of the ZQ63 alloy. The hydrogen release rate for the investigated alloys recorded in Dulbecco's medium are lower than in the SBF medium, but the behaviour of the alloys is similar. We can say that Dulbecco's medium is less aggressive due to the amino acids in its composition that have a catalytic role in the corrosion process.

ACKNOWLEDGEMENTS: -
This work has been funded by the European Social Fund from the Sectoral Operational Programme Human Capital 2014-2020, through the Financial Agreement with the title "Training of PhD students and postdoctoral researchers in order to acquire applied research skills - SMART", Contract no. 13530/16.06.2022 - SMIS code: 153734.

REFERENCES:

[1] I. Antoniac et al. Magnesium-Based Alloys Used in Orthopedic Surgery. Materials (2022), 15(3), 1148.

Hematopoietic stem cell transplantation alters bone structure and influences bone homeostasis

Saß RA[1,2], Bucher CH[1,2], Na IK, Penack O, Duda GN[1,2], Schmidt-Bleek K[1,2]

[1]Julius Wolff Institut, BIH at Charité, Berlin, GE, [2] Berlin Center Regenerative Therapies, BIH at Charité, Berlin, GE, [3] Medizinische Klinik mit Schwerpunkt Hämatologie, Onkologie und Tumorimmunologie, Charité – Universitätsmedizin Berlin, Berlin, GE

INTRODUCTION: Allogeneic hematopoietic stem cell transplantation (HSCT) is a potentially curative therapy for patients with malignant and nonmalignant diseases. Graft versus host disease (GVHD) mediated by donor T cells and hampered immunity with increased risk for infections are major complications post-transplant. Interestingly, several studies have demonstrated a higher risk of osteoporosis or fractures after HSCT. However, the underlying cellular mechanisms of HSCT-bone interactions have not been studied. The aim of this project is to unravel underlying interactions between immune and bone cells that lead to changes in bone post HSCT.

METHODS: We have developed a mouse model for HSCT to investigate bone and changes within during graft versus host disease (GVHD). Compared were a) syn = control without GVHD after HSCT and b) allo = a group that developed acute GVHD. 20, 40 and 60 days after cell transfer animals were sacrificed and bones were harvested. Bones underwent radiological and histological analyses to quantify the phenotype. Then, primary human mesenchymal stromal cells and osteoblasts were stimulated to differentiate and analyzed in metabolic assays in an in vitro setting to mimic GVHD. From this in vitro setting, conditioned media from selected activated immune cells was added to examine their potential to influence bone homeostasis.

RESULTS: Femora of mice developing a strong GVHD after allogeneic HSCT showed a larger medullary area and thinner cortical bone in the diaphyseal as well as an increase in bone volume and trabecular number in the epiphyseal region revealing differences in the whole bone structure. Remarkably, no osteoblastic lining cells were detectable and osteoid formation was absent, indicating an impaired bone formation capacity due to the GVHD. Furthermore, deviating B cell numbers and distributions were found. The in vitro analyses demonstrated the involvement of immune cell signalling seen in impaired (T cells) or improved (B cells) osteogenesis.

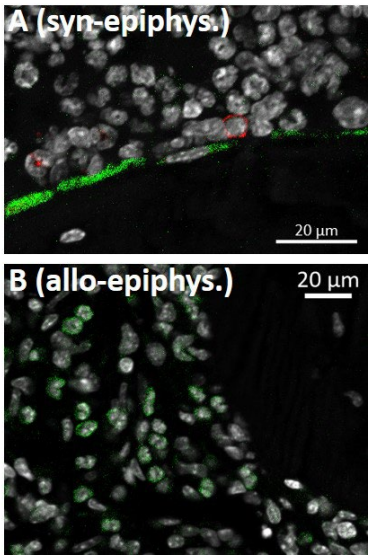

Fig. 1: Effect of different transplantations on Osteoblasts(green) and B cells(red): syngeneic (A) vs. allogeneic (B).

DISCUSSION & CONCLUSIONS: Impaired recovery of the immune system after allogeneic HSCT not only leads to an increased risk of severe infections. By examining bone structure in vivo and stroma cells in vitro we assume that the imbalance of immune cells of the adaptive immune system impedes the bone structure. This appears to be caused by a decreased capacity of osteogenic differentiation due to the lack of B cells. This discovery may be significant for the prognosis and treatment of long-term effects on the musculoskeletal tissue after HSCT.

ACKNOWLEDGEMENTS: This work was done with the help and support of the Bone Healing Group of the Julius-Wolff Institute, the groups of Il-Kang Na and Olaf Penack and received support from the Einstein Foundation ECRT.